Influence of fluctuations on the phase diagram of chiral nematic liquid crystals

J. Englert,[1] H. Stark,[1] L. Longa,[2] and H.-R. Trebin[1]
[1]*Institut für Theoretische und Angewandte Physik, Universität Stuttgart, Pfaffenwaldring 57, D-70550 Stuttgart, Germany*
[2]*Instytut Fizyki, Uniwersytet Jagielloński, Reymonta 4, Kraków, Poland*
(Received 16 July 1999)

In a recent paper [Phys. Rev. Lett. **81**, 1457 (1998)], we demonstrated that the phase diagram of the liquid crystalline blue phases, as calculated by means of Landau–de Gennes theory, displays serious deficiencies, which can only be removed if fluctuations are taken into account within statistical field theory. Here we present details of the calculations. The influence of fluctuations is treated self-consistently within a first order cumulant expansion. The square Δ of the inverse correlation length of the alignment tensor field is introduced as an order parameter. In a simplified model two phases of differing Δ appear at high chiralities, which are identified as the isotropic phase and the isostructural blue fog. The relationship between the cumulant expansion and the Brazovskiĭ method is illuminated.

PACS number(s): 64.70.Md, 05.40.−a, 61.30.Cz

I. INTRODUCTION

Blue phases [1] belong to the liquid crystalline state, but they display features of solids much more than any other liquid crystal. The centers of mass of the molecules do not exhibit positional order. In the cubic blue phases (BP's), however, the molecular axes align to form a complex long-range orientational pattern which is periodic along all three spatial directions. There are two cubic structures (BP I and BP II) of nonsymmorphic space groups O^2 (simple cubic) and O^8 (body-centered-cubic). Their lattice constants are about 500 nm, and they scatter light selectively in the visible spectrum. Defects, like dislocations, are directly observable in the microscope [2]. The range of existence of the blue phases is a few K. Thus they are thermodynamic phases, which are very difficult to synthesize and to stabilize. They are squeezed in between the high-temperature isotropic liquid and the low-temperature cholesteric phase. Recently, on the low-temperature side smectic and twist-grain boundary phases were also observed [3], and experimental evidence was provided for ''smectic blue phases'' [4]. The periodic order of BP II is melting directly into the isotropic phase or, at high chiralities, into a third blue phase (BP III). Due to its amorphous appearance, BP III is called ''blue fog.'' Only four years ago, it was established as an isotropic phase [5–7]. Unlike the cubic blue phases, its orientational order is correlated only over a few pitches of the cholesteric phase. All three blue phases are viscoelastic materials with finite shear modulus at zero frequency. The modulus continuously approaches zero in BP III, when it is heated toward the isotropic liquid [8]. Since the cubic blue phases break the continuous translational symmetry of the isotropic liquid, they exhibit hydrodynamic Goldstone modes equivalent to acoustic phonons in crystals. In Ref. [9] it was demonstrated that they can be viewed as a pure displacement of the local alignment tensor. The properties of these displacement modes and their appearance in light scattering experiments were thoroughly studied in Ref. [10].

Stable structures and phase diagrams were primarily calculated by mean-field theories. Although confirming roughly the phase sequence, the mean-field calculations disagree in many aspects with the experimental results. Until recently the best phase diagram was obtained by Grebel *et al.* (see Fig. 1) [11]. Using a Ginzburg–Landau–de Gennes free energy, they could explain the structure of the body-centered-cubic blue phase I with space group O^8 ($I4_132$) and the simple cubic blue phase II with space group O^2 ($P4_232$). Near the phase transition to the isotropic phase, instead of BP III they predicted a second body centered structure with space group O^5 ($I432$), which always condenses before O^2 and O^8 (see Fig. 2). Furthermore, they did not reproduce the experimentally well established disappearance of the BP II for high chiralities.

Many extensions of the mean-field theory were presented, taking regard of higher order terms [12] and secondary order parameters [13] in the free energy. However, the inconsistencies of the phase diagrams could not be resolved completely. Already at the early stage it was noted, that ''neglecting the fluctuations . . . may be a bad approximation'' [14]. On the other hand, it was claimed that ''fluctuations almost undoubtedly are irrelevant at phase transitions of weak crystallization into blue phases'' [15].

Experimentally, the situation is quite clear now. The universality of the phase diagrams as sketched in Fig. 3 and first documented by Yang and Crooker [16], has been confirmed many times. It seems to apply even to discotic systems [17]. Very recent measurements of specific heat, rotatory power, and light scattering [5–7] revealed evidence of a critical

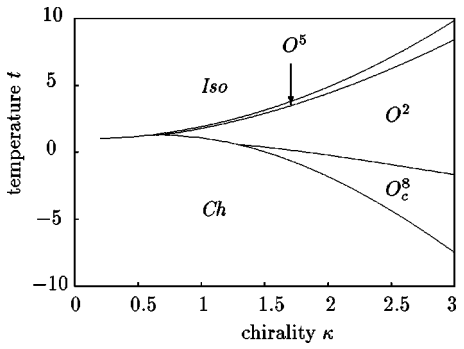

FIG. 1. Phase diagram recalculated from Landau–Ginzburg–de Gennes theory of Grebel *et al.* [11].

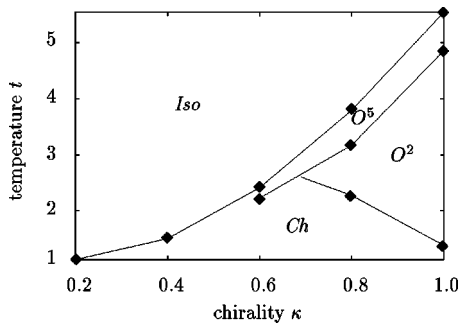

FIG. 2. One of the first mean-field phase diagrams of the blue phases (recalculated partial magnification of Fig. 1 of Grebel *et al.* [11]). Diamonds correspond to computed points in the phase diagram, and the solid lines are linear interpolations. Apart from the cholesteric phase and the O^5 structure no further phase shows a direct transition to the isotropic phase.

point terminating the first-order phase transition line between BP III and the isotropic phase.

In the meantime there is no doubt that BP III is a second isotropic phase, and the critical point is of the same universality class as the liquid-gas transition [18,19]. Calculations of the BP III–isotropic transition using a pseudoscalar order parameter [18,20] have shown how in principle such a critical point could be produced from the Landau–de Gennes Hamiltonian.

To take fluctuations into account, we go beyond mean-field theory and apply statistical field theory. The partition sum is evaluated approximately with the help of a cumulant expansion. We arrive naturally at a new order parameter, the square Δ of the inverse correlation length of the alignment tensor. It helps to discern two isotropic liquids at high chiralities, of which we interpret the strongly correlated one as BP III, and the weakly correlated one as the standard isotropic nematic.

The paper is organized as follows: After a short introduction into the theoretical description of the blue phases in Sec. II, new mean-field results are presented in Sec. III, which will help to understand the effects of fluctuations. In Sec. IV the cumulant expansion is explained. The relation to the so-called Brazovskiĭ method [21] is discussed briefly. In Sec. V we document the influence of fluctuations on the phase diagrams. Sections VI and VII are devoted to the isotropic phase. To obtain evidence for a transition between two isotropic phases, a third-order cumulant expansion has to be employed which we illustrate for a simplified model. In Sec. VIII the limitations of the theory are discussed.

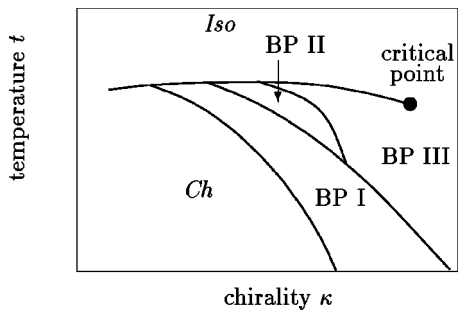

FIG. 3. Sketch of the experimental phase diagram of chiral nematic liquid crystals; κ and t are in arbitrary units.

II. THEORETICAL MODEL

The orientational order of the molecules in the blue phases is best described by the symmetric and traceless alignment tensor field $\mathbf{Q}(\mathbf{r})$. It can be expanded into spin tensor modes of $L=2$ and into plane waves, which yields

$$\mathbf{Q}(\mathbf{r})=\sum_{\mathbf{k}}\sum_{m=-2}^{2} Q_m(k)\mathbf{M}_m(\hat{\mathbf{k}})\mathrm{e}^{-\mathrm{i}\mathbf{k}\cdot\mathbf{r}}. \tag{1}$$

$k=|\mathbf{k}|$ is the modulus of $\mathbf{k}$, $\mathbf{M}_m(\hat{\mathbf{k}})$, $m=-2,\ldots,2$ are the base tensors, and $Q_m(k)$ is the Fourier amplitude of the mode $(\mathbf{k},m)$.

The Landau–Ginzburg–de Gennes Hamiltonian of chiral liquid crystals reads in real space [11],

$$H=H_2+H_3+H_4, \tag{2}$$

with

$$H_2=\frac{1}{2V}\int d^3r\,(aQ_{ij}Q_{ji}+c_1Q_{ij,l}Q_{ij,l}+c_2Q_{ij,i}Q_{lj,l}-2d\epsilon_{ijl}Q_{in}Q_{ln,j}),$$

$$H_3=-\frac{\beta}{\sqrt{24}V}\int d^3r\,Q_{ij}Q_{jk}Q_{ki},$$

$$H_4=\frac{\gamma}{24V}\int d^3r(Q_{ij}Q_{ji})^2,$$

where V is the system volume. In reciprocal space the Hamiltonian is written as

$$\begin{aligned}\mathcal{H}=&\frac{1}{4}\sum_{\mathbf{k}}\sum_{m}\left\{t-m\xi_R\kappa k+\xi_R^2\left[1+\frac{1}{6}\rho(4-m^2)\right]k^2\right\}\\&\times\mu_m(k)\mu_m(k)\\&-\frac{1}{2}\sum_{\mathbf{k}_1,\mathbf{k}_2,\mathbf{k}_3}\sum_{m_1,m_2,m_3}\mu_{m_1}(k_1)\mu_{m_2}(k_2)\mu_{m_3}(k_3)\\&\times\mathrm{Tr}[\mathbf{M}_{m_1}(\hat{\mathbf{k}}_1)\mathbf{M}_{m_2}(\hat{\mathbf{k}}_2)\mathbf{M}_{m_3}(\hat{\mathbf{k}}_3)]\delta_{\mathbf{k}_1+\mathbf{k}_2+\mathbf{k}_3,\mathbf{0}}\\&+\frac{1}{24}\sum_{\mathbf{k}_1,\mathbf{k}_2,\mathbf{k}_3,\mathbf{k}_4}\sum_{m_1,m_2,m_3,m_4}\\&\times\mu_{m_1}(k_1)\mu_{m_2}(k_2)\mu_{m_3}(k_3)\mu_{m_4}(k_4)\delta_{\mathbf{k}_1+\mathbf{k}_2+\mathbf{k}_3+\mathbf{k}_4,\mathbf{0}}\\&\times\mathrm{Tr}[\mathbf{M}_{m_1}(\hat{\mathbf{k}}_1)\mathbf{M}_{m_2}(\hat{\mathbf{k}}_2)]\mathrm{Tr}[\mathbf{M}_{m_3}(\hat{\mathbf{k}}_3)\mathbf{M}_{m_4}(\hat{\mathbf{k}}_4)],\end{aligned} \tag{3}$$

where we used dimensionless variables by defining

$$s=\beta/\sqrt{6}\gamma,\quad \mu_m(k)=Q_m(k)/s,\quad \mathcal{H}=\gamma s^4H, \tag{4}$$

$$a=\frac{\gamma s^2}{2}t\propto(T-T_0)/T_0,\quad \xi_R=\sqrt{\frac{2c_1}{s^2}}, \tag{5}$$

$$\kappa=\frac{\xi_R}{c_1}d, \quad \rho=\frac{c_2}{c_1}. \tag{6}$$

The amplitudes differ by a factor of $\sqrt{N}/\sqrt{24}$, and the Hamiltonian by a factor of 24 compared to Ref. [11]. N is the number of prongs in the star of wave vectors for a given modulus of $\mathbf{k}$.

III. NEW MEAN-FIELD RESULTS

The mean-field free energy is obtained by substituting equilibrium values $\bar{\mu}_m(k)$ of the amplitudes into Eq. (3). The results of Grebel *et al.* [11] then follow from a minimization of the free energy with respect to these amplitudes. While Grebel *et al.* only kept $m=2$ modes we also checked the influence of modes $m\neq 2$, to see whether their neglect causes the deficiencies of the mean-field calculations. The $m=\pm 1$ components of the first star are forbidden by selection rules [11]. The $m=-2$ component is strongly depressed compared to $m=2$ by choice of a positive handedness. As a simple test we calculated mean-field phase diagrams with $m=2$ components for all stars, and an additional $m=0$ component for the first star only. In the following we use a notation similar to Grebel *et al.* [11]: μ_0 is the $m=0$ Fourier component of the first star, μ_j, $j=1,2,4,6$, and 8 are the $m=2$ Fourier components of successive stars. For the O^2 structure we take only two stars into account, (100) with an amplitude $\bar{\mu}_1$, and (110) with $\bar{\mu}_2$. For the O^5 structure there are three stars: (110), $\bar{\mu}_2$; (112), $\bar{\mu}_6$; and (220), $\bar{\mu}_8$. For the O^8 structure, finally, there is an additional star (200), $\bar{\mu}_4$.

The complete list of mean-field free energies is found in Ref. [22]. Here we present the main results only. The free energy of the O^2 structure reads

$$\mathcal{H}_{O^2}=\mathcal{H}_{O^2}^{\mathrm{GHS}}+\frac{3}{2}[t+\kappa^2(1+2\rho/3)r_{O^2}^2]\bar{\mu}_0^2+g(\mu_k)\bar{\mu}_0^2+\frac{9}{4}\bar{\mu}_0^4, \tag{7}$$

where r_{O^2} is the lattice constant [11] and $g(\bar{\mu}_k)$ is a positive definite function of the $\bar{\mu}_k$. It is globally minimized by $\bar{\mu}_0=0$, since $g(\mu_k)$ is always larger than the temperature dependent term. The free energy of the O^8 structure also possesses cubic contributions in $\bar{\mu}_0$. For small chiralities and low temperatures, where BP I is only metastable, we find that $\bar{\mu}_0\neq 0$ can occur. However, in the whole range of stability of BP I, the free energy is minimized by $\bar{\mu}_0=0$. For the O^5 structure, the free energy contains linear terms in $\bar{\mu}_0$ which consequently cannot vanish and enhance the stability of the phase. The changes in the phase diagram, however, are negligibly small. We, therefore, assume that the only relevant terms are indeed the $m=2$ contributions.

We have investigated the behavior of the mean-field phase diagram for very high chiralities ($\kappa>3$, Fig. 4). The phase transition line between $O^8_{c/b}$ and O^2 has a minimum at $\kappa\approx 5$. At the same value of κ a reentrant O^8_d phase arises, which causes the O^2 structure to vanish at $\kappa\approx 12$. In Sec. V we will show that the reentrant O^8_d phase is an artifact of the mean-field theory. The disappearance of the O^2 structure due to fluctuations occurs at lower chiralities.

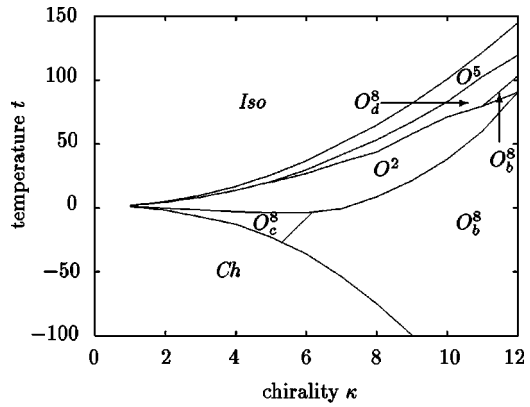

FIG. 4. Mean-field phase diagram of the blue phases for $\kappa\leqslant 12$.

The O^8 structure undergoes an isostructural transition from O^8_c ($\bar{\mu}_2\approx\bar{\mu}_4$, $\bar{\mu}_6/\bar{\mu}_2\approx 0.3$, $\bar{\mu}_8/\bar{\mu}_2<0.06$, $\bar{\mu}_2>0$, $\bar{\mu}_4>0$) to O^8_b, where the second harmonic is very small ($\bar{\mu}_4/\bar{\mu}_2\lesssim 0.15$, $\bar{\mu}_2>0$, $\bar{\mu}_4>0$). The reentrant O^8_d phase possesses a very small first harmonic ($\bar{\mu}_2/|\bar{\mu}_4|\lesssim 0.2$, $\bar{\mu}_2>0$, $\bar{\mu}_4<0$).

Chiralities above $\kappa\approx 2$ were declared unphysical by Grebel *et al.* [11]. We would like to mention, however, that the role of the chirality parameter κ is not quite clear. The pitch, which is proportional to κ, is known to depend strongly on temperature [23], but κ is chosen temperature independent. In experimental phase diagrams the pitch is determined for a single temperature only just below the clearing point [16]. The relevant quantity is rather the temperature independent mole fraction of the chiral compound, and it is not excluded that high chirality values, i.e., $\kappa>3$, are physically relevant.

IV. CUMULANT EXPANSION

A. Application to blue phases

To incorporate fluctuations of the order parameter into the calculations of the phase diagram of the blue phases we start from the statistical definition of the free energy

$$F=-\beta^{-1}\ln Z=-\beta^{-1}\ln\int D\mu\,\exp(-\beta\mathcal{H}[\mu]), \tag{8}$$

$\beta=1/k_BT$, which we evaluate with the help of the cumulant expansion. With respect to phase transitions, the cumulant expansion was originally used in the renormalization group scheme [24], and recently applied to block copolymers [25].

The order parameter $\mu=\bar{\mu}+\mu'$ is subdivided into an equilibrium part $\bar{\mu}$ and a fluctuating part μ'. The path integration then has to be carried out over all smooth paths μ'. We rewrite the Hamiltonian as

$$\mathcal{H}[\mu]=\mathcal{H}[\bar{\mu}]+\tilde{\mathcal{H}}[\bar{\mu},\mu']=F^{\mathrm{MF}}[\bar{\mu}]+\tilde{\mathcal{H}}[\bar{\mu},\mu'], \tag{9}$$

where $F^{\mathrm{MF}}[\bar{\mu}]$ is the mean-field free energy.

The path integral in Eq. (8) cannot be solved analytically. For the fluctuations, therefore, we choose a Gaussian trial Hamiltonian

$$\mathcal{H}'[\mu']=\frac{1}{4}\sum_{\mathbf{q}}\left[\Delta+(q-\kappa)^2\right]\mu'_{\mathbf{q}}\mu'_{-\mathbf{q}}, \tag{10}$$

with Δ, which represents a ''mass term'' or ''reduced temperature'' [cp. the quadratic part in Eq. (3)] as variational parameter. In the following we concentrate on fluctuations of the $m=2$ mode and denote the amplitude of the fluctuating mode ($m=2,\mathbf{k}=\mathbf{q}$) by $\mu'_{\mathbf{q}}$ and of the equilibrium part by $\overline{\mu}_{\mathbf{q}_i}$ or $\overline{\mu}_i$. The partition function corresponding to Hamiltonian (10) reads

$$Z'=\int D\mu' \exp(-\beta\mathcal{H}'[\mu']). \tag{11}$$

With Eqs. (10) and (11) we rewrite Eq. (8) as

$$F=F^{\mathrm{MF}}[\overline{\mu}] -\beta^{-1}\ln\left[\left(\int D\mu' e^{-\beta(\tilde{\mathcal{H}}[\overline{\mu},\mu']-\mathcal{H}'[\mu'])}e^{-\beta\mathcal{H}'[\mu']}\right)\frac{Z'}{Z'}\right], \tag{12}$$

which simplifies to

$$F=\mathcal{H}[\overline{\mu}]-\beta^{-1}\ln\langle e^{-\beta(\tilde{\mathcal{H}}[\overline{\mu},\mu']-\mathcal{H}'[\mu'])}\rangle_{\mathcal{H}'}-\beta^{-1}\ln Z'. \tag{13}$$

All expectation values are now calculated with respect to $\mathcal{H}'[\mu']$ indicated by the subscript index. We define $\delta\mathcal{H}=\tilde{\mathcal{H}}[\overline{\mu},\mu']-\mathcal{H}'[\mu']$ and expand the second term into a Taylor series. It yields up to third order in $\delta\mathcal{H}$:

$$\ln\langle e^{-\beta(\tilde{\mathcal{H}}[\overline{\mu},\mu']-\mathcal{H}'[\mu'])}\rangle=-\beta\langle\delta\mathcal{H}\rangle+\frac{\beta^2}{2}(\langle\delta\mathcal{H}^2\rangle -\langle\delta\mathcal{H}\rangle^2)-\frac{\beta^3}{6}(\langle\delta\mathcal{H}^3\rangle-3\langle\delta\mathcal{H}\rangle \times\langle\delta\mathcal{H}^2\rangle+2\langle\delta\mathcal{H}\rangle^3) +O(\langle\delta\mathcal{H}^4\rangle). \tag{14}$$

All terms of the same order in $\delta\mathcal{H}$ are called moments or cumulants of $\delta\mathcal{H}$. In a first-order approximation the free energy then reads

$$F=F^{\mathrm{MF}}[\overline{\mu}]-\beta^{-1}\ln Z'+\langle\tilde{\mathcal{H}}[\overline{\mu},\mu']-\mathcal{H}'[\mu']\rangle_{\mathcal{H}'}. \tag{15}$$

To arrive at the free energies for different structures we have to calculate the last two terms of Eq. (15) explicitly. First, we need the definition of the two-particle correlation function and of the self energy function.

The two-particle correlation function, corresponding to the trial Hamiltonian of Eq. (10), is given by

$$\langle\mu'_{\mathbf{q}}\mu'_{-\mathbf{q}}\rangle_{\mathcal{H}'}=\frac{2\beta^{-1}}{\Delta+(q-\kappa)^2}=\beta^{-1}\chi(\mathbf{q}), \tag{16}$$

where we have introduced the wave vector dependent susceptibility $\chi(\mathbf{q})$ of $\overline{\mu}_{\mathbf{q}}$ [24]. $\Delta^{-1/2}$ is the correlation length of the alignment tensor field. The integral over the correlation function,

$$\frac{1}{4}\sum_{\mathbf{q}}\langle\mu'_{\mathbf{q}}\mu'_{-\mathbf{q}}\rangle_{\mathcal{H}'}=\frac{V\beta^{-1}}{4\pi^2}\int_0^{n\kappa}\frac{q^2dq}{\Delta+(q-\kappa)^2}=\Sigma(\Delta), \tag{17}$$

is called the self-energy function. It can be evaluated analytically:

$$\Sigma(\Delta)=\frac{V\beta^{-1}}{4\pi^2}\kappa\left\{n-\ln\left(\frac{1+\kappa^2/\Delta}{1+(\kappa^2/\Delta)(n-1)^2}\right) -\frac{\sqrt{\Delta}}{\kappa}\left(1-\frac{\kappa^2}{\Delta}\right)\left[\arctan\left(\frac{\kappa}{\sqrt{\Delta}}\right) +\arctan\left(\frac{\kappa}{\sqrt{\Delta}}(n-1)\right)\right]\right\}. \tag{18}$$

We will comment below about the cutoff radius $n\kappa$ in Eq. (17). Higher-order correlation functions are simplified using Wick's theorem [24].

Now we present details of the calculation of $\langle\delta\mathcal{H}\rangle_{\mathcal{H}'}$. The third term of Eq. (15) comes from the quartic invariant, and contains terms of the form

$$\frac{1}{6}\sum_i(1+2\lambda_{ij,-i,-j})\langle\mu'_{\mathbf{q}_i}\mu'_{-\mathbf{q}_i}\rangle, \tag{19}$$

where $\lambda_{ijkl}=\mathrm{Tr}[\mathbf{M}(\hat{\mathbf{k}}_i)\mathbf{M}(\hat{\mathbf{k}}_j)]\mathrm{Tr}[\mathbf{M}(\hat{\mathbf{k}}_k)\mathbf{M}(\hat{\mathbf{k}}_l)]$. The angular part of the integral can be calculated according to

$$\frac{1}{4\pi}\int_0^{2\pi}\int_0^{\pi}(1+2|\mathrm{Tr}[\mathbf{M}_2(\hat{\mathbf{q}})\mathbf{M}_2(\hat{\mathbf{k}})]|^2)\sin\theta d\theta d\varphi =\frac{1}{4\pi}\int_0^{2\pi}\int_0^{\pi}\left(1+2\sin^8\frac{\theta}{2}\right)\sin\theta d\theta d\varphi=\frac{7}{5}, \tag{20}$$

where θ is the angle between $\mathbf{k}$ and $\mathbf{q}$. The cubic contribution of $\langle\delta\mathcal{H}\rangle_{\mathcal{H}'}$ vanishes according to

$$3\overline{\mu}_0\sum_i\beta_{i,-i,0}\langle\mu'_{\mathbf{q}_i}\mu'_{-\mathbf{q}_i}\rangle=0 \tag{21}$$

with $\beta_{ijk}=\mathrm{Tr}[\mathbf{M}(\hat{\mathbf{k}}_i)\mathbf{M}(\hat{\mathbf{k}}_j)\mathbf{M}(\hat{\mathbf{k}}_k)]$.

The self-energy function follows from the derivative of Z' with respect to Δ:

$$\frac{\partial Z'}{\partial\Delta}=-\beta Z'\Sigma(\Delta). \tag{22}$$

After integration, we obtain

$$-\beta^{-1}\ln Z'=\int_0^{\Delta}\Sigma(\Delta')d\Delta'. \tag{23}$$

The final expression for the free energy within the first-order cumulant expansion reads

$$F = F^{\mathrm{MF}}[\bar{\mu}] + \int_0^{\Delta} \Sigma(\Delta')\, d\Delta' + \left(\tau - \Delta + \frac{14}{15}\Sigma(\Delta) + \frac{7}{15} \sum_i \bar{\mu}_i \bar{\mu}_{-i} \right) \Sigma(\Delta). \quad (24)$$

In order to obtain phase diagrams the free energy, Eq. (24), has to be minimized with respect to the variational parameters Δ and $\bar{\mu}$. Variation with respect to Δ leads to a Dyson type equation

$$-\Delta + \tau + \frac{28}{15}\Sigma(\Delta) + \frac{7}{15} \sum_i \bar{\mu}_i \bar{\mu}_{-i} = 0, \quad (25)$$

which is the determining equation for Δ. The free energy of Eq. (24) can be simplified with the help of Eq. (25):

$$F = F^{\mathrm{MF}}[\bar{\mu}] + \int_0^{\Delta} \Sigma(\Delta')\, d\Delta' - \frac{14}{15}\Sigma^2(\Delta). \quad (26)$$

In Sec. V we will use Eqs. (25) and (26) to numerically compute phase diagrams of the blue phases.

B. Connection with the Brazovskiĭ method

Here we would like to clarify the connection between the cumulant expansion and the Brazovskiĭ method [15,21]. Brazovskiĭ and co-workers calculated the Dyson equation for ordered structures, assuming that

$$\frac{\delta F}{\delta \bar{\mu}_{-\mathbf{q}_i}} = \left\langle \frac{\delta \mathcal{H}[\bar{\mu}, \mu']}{\delta \bar{\mu}_{-\mathbf{q}_i}} \right\rangle_{\mathcal{H}'}. \quad (27)$$

The two point vertex function is given by

$$\beta^{-1} \Gamma^{(2)}_{i,-i} = \frac{\delta^2 F}{\delta \bar{\mu}_{\mathbf{q}_i} \delta \bar{\mu}_{-\mathbf{q}_i}}, \quad (28)$$

and is proportional to the inverse two point correlation function. The resulting self-consistent equation represents the Dyson equation for ordered structures.

Applying this method to blue phases, we obtain the following Dyson equation instead of Eq. (25):

$$-\Delta + \tau + 6\bar{\mu}_0(\beta_{-j,j,0} + \beta_{j,-j,0}) + \frac{1}{3} \sum_i \bar{\mu}_i \bar{\mu}_i (1 + 2\lambda_{i,j,-i,-j}) + \frac{28}{15}\Sigma(\Delta) = 0, \quad (29)$$

where λ_{ijkl} and β_{ijk} are defined as in Eqs. (19) and (21). The free energy is exactly the same as Eq. (26). The index j of Eq. (29) corresponds to the equilibrium amplitude $\bar{\mu}_j$ of the first star.

It is evident, that the Dyson equation (29) for the isotropic phase is equivalent to Eq. (25). For the ordered structures, however, it differs: In Brazovskiĭ's method the term $(1 + 2\lambda_{i,j,-i,-j})$ has to be summed over the star $\mathbf{k}_i$, and j, as noted, corresponds to an equilibrium value. Thus, even if $\bar{\mu}_j$ vanishes for some reason, Eq. (29) still depends on j via the tensor components $\beta_{-j,j,0}$ and $\beta_{j,-j,0}$, as for example in the case of O^2. Since O^8 is a subgroup of the former, the free energy of O^2 can usually be obtained by setting the amplitudes of the first and third stars of O^8 to zero. This property, however, is not reflected by the Dyson equation (29). Instead, since j belongs to the first star of O^8 the procedure leads to an O^2 structure with fluctuations around a (110) star. In the Dyson equation derived for the O^2 structure, on the other hand, one arrives at fluctuations around the (100) star. Consequently, two different Dyson equations for O^2 can be derived, which is a source of inconsistencies.

Even worse, the linear term proportional to $\bar{\mu}_0(\mathbf{k}=\mathbf{0})$ produces an effective linear term in the free energy,

$$\frac{dF}{d\bar{\mu}_i} = \frac{\partial F}{\partial \bar{\mu}_i} + \frac{\partial F}{\partial \Delta} \frac{\partial \Delta}{\partial \bar{\mu}_i}, \quad (30)$$

making the isotropic phase unstable. For the cholesteric phase there is an $m=0$ mode with $\mathbf{k}=\mathbf{0}$; thus, with Eqs. (26) and (29),

$$\frac{dF}{d\bar{\mu}_0} = \frac{\partial F^{\mathrm{MF}}}{\partial \bar{\mu}_0} - \sqrt{6}\Sigma(\Delta). \quad (31)$$

The condition for the isotropic phase to be stable is that first derivative of the free energy with respect to the equilibrium order parameter vanishes for all equilibrium order parameters set to zero. Here, however,

$$\frac{dF}{d\bar{\mu}_0} = -\sqrt{6}\Sigma(\Delta) \neq 0, \quad (32)$$

since the self-energy function is nonzero everywhere. In conclusion we point out, that Brazovskiĭ's method is different from the cumulant expansion even in first order, and yields misleading results in the case of blue phases.

V. PHASE DIAGRAMS

A. Influence of fluctuations

Apart from temperature and chirality there are two other parameters present in the free energy [Eq. (26)]: the cutoff radius n and the energy scale of the fluctuations $\beta^{-1} = k_B T$, where T is close to the clearing point temperature. Let us introduce the convenient quantity $\alpha = \beta^{-1} V/(60\pi^2)$. First we will present phase diagrams with fixed $n=1$ and increasing α. Second, we discuss the role of the cutoff radius.

Let us summarize the main deficiencies of the mean field phase diagram: The cubic structure O^5, that has not been observed experimentally, appears at the phase transition between the cubic phases and the isotropic phase before any other cubic structure can condensate. Hence neither O^2 nor O^8 show a direct phase transition to the isotropic phase. There is no model of the blue fog included in the mean-field calculations of Ref. [11].

In Fig. 5 we show what happens to the mean-field phase diagram when the fluctuations are turned on weakly. From Eqs. (26) and (18) we obtain the mean-field phase diagram by putting $\alpha=0$, as sketched with solid lines in Fig. 5. On

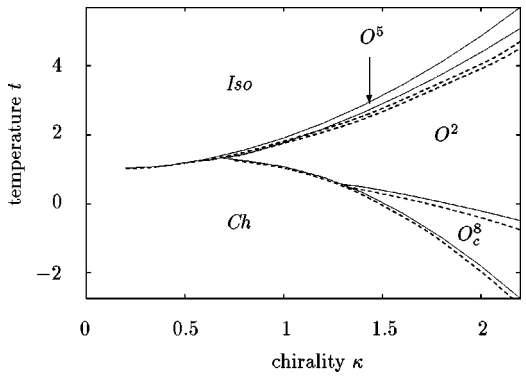

FIG. 5. The solid lines of the phase diagram represent the mean-field behavior. If fluctuations are included, the transition lines change, as illustrated by the dashed lines. Note that the O^5 phase has almost vanished from the phase diagram. The strength of the fluctuations is characterized by $\alpha=0.025$, and only the first shell $(n=1)$ is included.

increasing α the phase transition line to the isotropic phase is bent downwards, whereas the other transition lines are influenced less the farther away they are from the clearing point. The structure which is most affected by fluctuations is the O^5 structure. In Fig. 5 it can be clearly seen that the range of stability of O^5 has shrunk dramatically.

Furthermore, the effect of fluctuations increases with increasing chirality κ, as can be understood from Eq. (18): For high chiralities, $\Delta \ll \kappa^2$, $\Sigma(\Delta)$ increases as $\kappa^2/\sqrt{\Delta}$, as long as $\kappa^2/\Delta \gg n^2$ $(n \lesssim 5)$. In the latter case, $\Sigma(\Delta)$ will be almost independent of Δ and behave like $n\kappa$. For small chiralities, on the other hand, $\Delta \gg \kappa^2$, $\Sigma(\Delta)$ decreases as $n^2\kappa^3/\Delta$.

At $\alpha \gtrsim 0.075$ the O^5 structure has disappeared completely from the phase diagram. In Fig. 6 we plot phase diagrams for further increase of α. For $\alpha=0.2$ the phase transition line to the isotropic phase is bent down [see Fig. 6(a)]. For $\alpha=0.5$ the range of stability of the blue phases is very small. O^2 disappears for chiralities $\kappa \gtrsim 2$ [see Fig. 6(b)]. Increasing α further to 0.7, O^2 completely disappears from the phase diagram, and the range of stability for O^8 is shifted to even higher chiralities.

The disappearance of the O^2 structure for high chiralities is a universal feature for the phase diagrams of chiral-nematic liquid crystals. In Sec. III we have already seen that it also happens in the mean-field diagram, though for chiralities larger than 12. With increasing α the point where O^2 vanishes shifts to smaller chiralities, and the phase transition line to the isotropic phase is moved to lower temperatures, where it eventually crosses the O^8-O^2 phase transition line. The phase diagram which agrees best with the experimental one is obtained for $\alpha=0.2$ (Fig. 7, which is the continuation of Fig. 6 to an extended range of chiralities).

B. Cutoff radius

How do the results change when the cutoff radius $n\kappa$ is increased? For small κ the self energy integral is proportional to αn^2. Choosing $n=2$, we must divide α by 4 to obtain results with equal strength of fluctuations. This is illustrated in Fig. 8, which has to be compared to Fig. 6(a). For $n=3$ and $\alpha=0.03$, the phase diagram is very similar to Fig. 8.

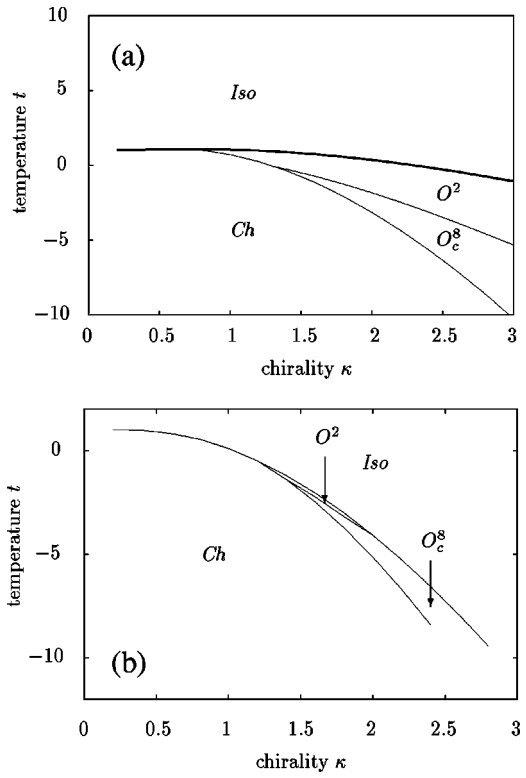

FIG. 6. Phase diagram of the blue phases for different parameters α and $n=1$. (a) $\alpha=0.2$. The bold line corresponds to the bold line of Fig. 10. (b) $\alpha=0.5$.

The qualitative behavior does not change too much when n is increased up to 3. For $n=4$ (Fig. 9) a difference is already visible. Although there is still no O^5 structure present, the phase transition line rises again for $\kappa \gtrsim 2.5$, widening the range of stability of O^2, in disagreement with the experiment. For $n \approx 10$ the O^5 structure is back again. Consequently, there should be an upper limit for the cutoff radius.

From physical considerations the necessity for a cutoff is evident. The order parameter $\mathbf{Q}(\mathbf{r})$ is an average on a mesoscopic scale of several hundred ångstroms. Assuming a molecular length of about 20 Å, the mesoscopic scale corresponds to ten times the molecular length. For $n=1$ only fluctuations with wave lengths greater than the lattice constant are taken into account. Increasing n we add step by step

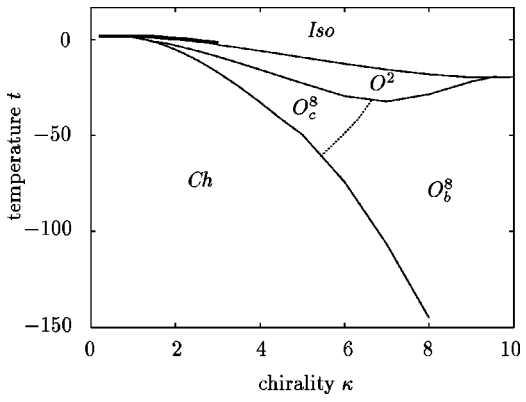

FIG. 7. Phase diagram of the blue phases for $\kappa \leqslant 10$, $\alpha=0.2$, and $n=1$.

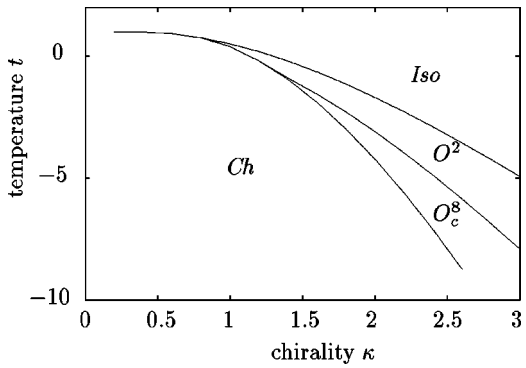

FIG. 8. Phase diagram of the blue phases for $\alpha = 0.05$ and $n = 2$.

shorter wavelength fluctuations. At $n = 10$ the mesoscopic scale, where the order parameter is defined is reached and the theory breaks down.

From Eq. (18) we recognize that for higher n the term proportional to $n\kappa$ (being the upper cutoff of the integral), which does not depend on Δ, dominates the self energy function and effectively suppresses long wavelength fluctuations. The short range fluctuations, on the other hand, should also contain contributions that are not described by a mesoscopic theory. In conclusion, we could show that, in a reasonable range for the cutoff radius, the qualitative results remain unchanged. For high n short range fluctuations dominate, which have no physical meaning.

VI. BEHAVIOR OF THE ISOTROPIC PHASE

In mean-field theory the free energy of the isotropic phase equals zero, but not when fluctuations are taken into account. In Fig. 10 the solution of Eq. (25) for the inverse coherence length $\sqrt{\Delta}$ in the isotropic phase is plotted versus temperature t for different κ. Clearly, two different regimes can be recognized for small chiralities: one at low temperatures where $\sqrt{\Delta}$ is small, and another where $\sqrt{\Delta}$ is about two orders of magnitude larger. The regimes are connected smoothly. It is a phase behavior, where an order parameter changes its value rapidly over the ordering field (the temperature) but behaves continuously in all derivatives. The smooth transition vanishes for increasing κ.

In Sec. IV we have argued that $\Delta^{-1/2}$ is the correlation length of the alignment tensor or, respectively, the inverse

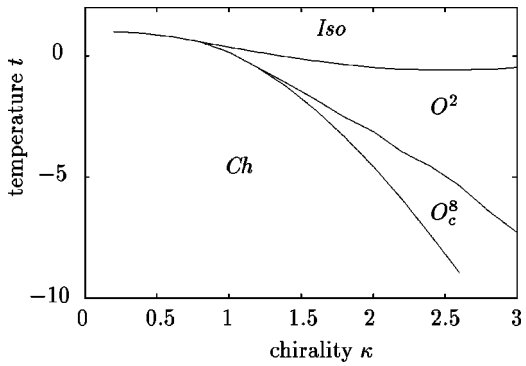

FIG. 9. Phase diagram of the blue phases for $\alpha = 0.012$ and $n = 4$.

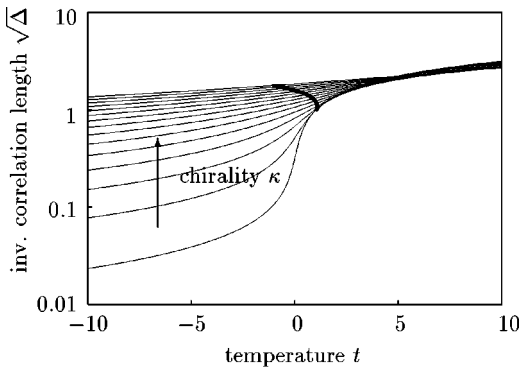

FIG. 10. Inverse correlation length $\sqrt{\Delta}$ vs temperature t for chirality κ between 0.2 and 3.0. The area on the right side of the bold line is the regime for the stable isotropic phase, and the area on the left side is that for the metastable state. The bold line corresponds to the bold line of Fig. 6(a).

susceptibility. Consequently, in the low-temperature region there is a strongly correlated isotropic phase, whereas in the high-temperature region it is weakly correlated. This is a hint of a second isotropic phase, and the high chirality behavior indicates the existence of a critical point. An appropriate thermodynamic order parameter is the inverse susceptibility.

It has to be stressed that there is no real phase transition within the first-order cumulant expansion. It can be shown [22] that the situation does not change when modes other than $m = 2$ are added. The corresponding equation must be at least of third order in t to provoke a van der Waals like behavior. For a phase transition the condition $\partial t/\partial\Delta < 0$ is necessary in some interval $[\Delta_1, \Delta_2]$, implying an instability.

For convenience the line where ordered structures become stable is plotted, too, in Fig. 10. On the right side of the bold line the isotropic phase is stable, whereas on the left it is only metastable. The isotropic phase obtained in the preceding phase diagrams has therefore always been the ''true'' weakly correlated isotropic phase.

VII. THIRD-ORDER CUMULANT EXPANSION IN A SIMPLIFIED MODEL

From the remarks of the last section it is clear, that we can only obtain an isostructural BP III–isotropic phase transition if we extend our theory to a third-order cumulant expansion. Unfortunately, such an expansion is a very tedious work for the Hamiltonian of the blue phases. To check whether chiral systems provide a second isotropic phase and a critical point, we simplified the problem by neglecting the cubic contribution to the Hamiltonian and by setting all base matrices $\mathbf{M}(\hat{\mathbf{k}})$ equal to unity. We then are left with a chiral ϕ^4 theory.

Both limitations should not change the qualitative behavior of the system, since to first order the cubic term did not contribute to the fluctuating part of the free energy, and the traces only appeared in angular integrals yielding numerical constants. Both issues will change in a higher order theory, but the simplified model should provide a guideline.

For the remaining calculations we start from the Hamiltonian

$$\mathcal{H}[\phi]=\frac{1}{2}\sum_{\mathbf{q}}\,[t+(q-q_0)^2]\phi_{\mathbf{q}}\phi_{-\mathbf{q}} + \frac{\lambda}{4!}\sum_{\mathbf{q}_1+\mathbf{q}_2+\mathbf{q}_3+\mathbf{q}_4=\mathbf{0}}\phi_{\mathbf{q}_1}\phi_{\mathbf{q}_2}\phi_{\mathbf{q}_3}\phi_{\mathbf{q}_4}, \tag{33}$$

where $\overline{\phi}$ and ϕ' are the equilibrium and fluctuating part of the order parameter, respectively, and the Gaussian trial Hamiltonian reads

$$\mathcal{H}'[\phi']=\frac{1}{2}\sum_{\mathbf{q}}\,[\Delta+(q-q_0)^2]\phi'_{\mathbf{q}}\phi'_{-\mathbf{q}}. \tag{34}$$

q_0 is equivalent to the chirality κ.

Using a third-order cumulant expansion the free energy of the isotropic phase then reads

$$\begin{aligned}F=&\int\Sigma(\Delta')d\Delta'\\&+(t-\Delta)\Sigma\left(1-\beta\lambda\Pi+\beta^2\lambda^2X\Sigma+\frac{\lambda^2\beta^2}{12}\frac{\zeta_2}{\Sigma}\right)\\&-\frac{\beta}{2}(t-\Delta)^2\Pi\left(1-\beta\lambda\Pi-2\lambda\beta\frac{\Sigma X}{\Pi}\right)\\&+\frac{\beta^3}{3}(t-\Delta)^3X+\frac{\lambda}{2}\Sigma^2(1-\lambda\beta\Pi+\lambda^2\beta^2\Pi^2)\\&+\lambda^2\beta^2\Sigma\left(\frac{\lambda}{3}\Sigma^2X+\Pi^2\right)\\&-\frac{\lambda^2\beta}{48}(\rho-\lambda\beta\zeta_1-4\lambda\beta\Sigma\zeta_2).\end{aligned} \tag{35}$$

The following abbreviations are used:

$$\Sigma=\frac{1}{(2\pi)^2\beta}\int_0^{nq_0}\frac{q^2dq}{\Delta+(q-q_0)^2}, \tag{36}$$

$$\Pi=\frac{1}{(2\pi)^2\beta^2}\int_0^{nq_0}\frac{q^2dq}{[\Delta+(q-q_0)^2]^2}=-\beta^{-1}\frac{\partial\Sigma}{\partial\Delta}, \tag{37}$$

$$X=\frac{1}{(2\pi)^2\beta^3}\int_0^{nq_0}\frac{q^2dq}{[\Delta+(q-q_0)^2]^3}=\frac{1}{2\beta^2}\frac{\partial^2\Sigma}{\partial\Delta^2}, \tag{38}$$

and

$$G_{\mathbf{q}}=\langle\phi'_{\mathbf{q}}\phi'_{-\mathbf{q}}\rangle, \tag{39}$$

$$\rho=\sum_{\mathbf{k}_1\mathbf{k}_2\mathbf{k}_3}G_{\mathbf{k}_1}G_{\mathbf{k}_2}G_{\mathbf{k}_3}G_{-\mathbf{k}_1-\mathbf{k}_2-\mathbf{k}_3}, \tag{40}$$

$$\zeta_1=\sum_{\mathbf{k}_1\mathbf{k}_2\mathbf{k}_3\mathbf{k}'}G_{\mathbf{k}_1}G_{\mathbf{k}_2}G_{\mathbf{k}_3}G_{\mathbf{k}'}G_{-\mathbf{k}_1-\mathbf{k}_2-\mathbf{k}_3}G_{\mathbf{k}_1+\mathbf{k}_2-\mathbf{k}'}, \tag{41}$$

$$\zeta_2=\sum_{\mathbf{k}_1\mathbf{k}_2\mathbf{k}_3}G^2_{\mathbf{k}_1}G_{\mathbf{k}_2}G_{\mathbf{k}_3}G_{\mathbf{k}_1-\mathbf{k}_2-\mathbf{k}_3}. \tag{42}$$

The latter functions must be calculated numerically. A fit to the numerical data obtained by a standard Monte Carlo integration yields

$$\begin{aligned}\rho(\Delta,q_0)=&\frac{\beta^{-4}}{2^7\pi^8}(0.001\,15q_0^{-5}\Delta^2+0.0071q_0^{-6}\Delta^{2.5}\\&+0.111q_0^{-7}\Delta^3-0.049q_0^{-8}\Delta^{3.5}\\&+0.182q_0^{-9}\Delta^4)^{-1},\end{aligned} \tag{43}$$

$$\begin{aligned}\zeta_1=&(\beta^{-6}2^{-10}\pi^{-11})(0.000\,0252q_0^{-6}\Delta^3+0.0084q_0^{-8}\Delta^4\\&+0.023q_0^{-10}\Delta^5+0.0425q_0^{-12}\Delta^6)^{-1},\end{aligned} \tag{44}$$

$$\begin{aligned}\zeta_2=&(\beta^{-5}2^{-7}\pi^{-8})(0.002\,28q_0^{-5}\Delta^3+0.0103q_0^{-6}\Delta^{3.5}\\&+0.144q_0^{-7}\Delta^4-0.061q_0^{-8}\Delta^{4.5}+0.183q_0^{-9}\Delta^5)^{-1}.\end{aligned} \tag{45}$$

Equation (35) has been minimized numerically. The result is plotted in Fig. 11. For small values of q_0 there is a jump in the correlation length at $t\approx0.1$ [Figs. 11(a) and 11(b)]. In Fig. 11(b), which represents a close-up of Fig. 11(a), it can be clearly seen that the slope of $\Delta(t)$ is approximately the same and finite at both branches indicating a first-order phase transition.

For increasing q_0 the relative height of the jump decreases. At the same time the jump shifts toward higher temperatures [see Fig. 11(c)]. For $q_0\approx0.7$ the jump disappears, and the correlation length is continuous over the temperature, as illustrated in Fig. 11(d) for $q_0=0.8$. We have, thus, proven the existence of a critical point in a chiral ϕ^4 model. We note that a small maximum of $\Delta(t)$ is present at $t=0$, which might be an artifact of the third-order approximation.

Although the Hamiltonian used in this section is simplified compared to the Hamiltonian of the blue phases, we predict a qualitatively similar behavior for the blue phases. This prediction is supported by Fig. 12, where we plot Δ versus temperature on a linear scale. According to Eq. (16) Δ is proportional to the inverse intensity of the scattered light for a given chirality and wavelength of the incident light. Such measurements have been carried out by Koistinen and Keyes at the BP III–isotropic phase transition [6]. Our prediction calculated within the simplified model reveals a striking agreement with the experimental data.

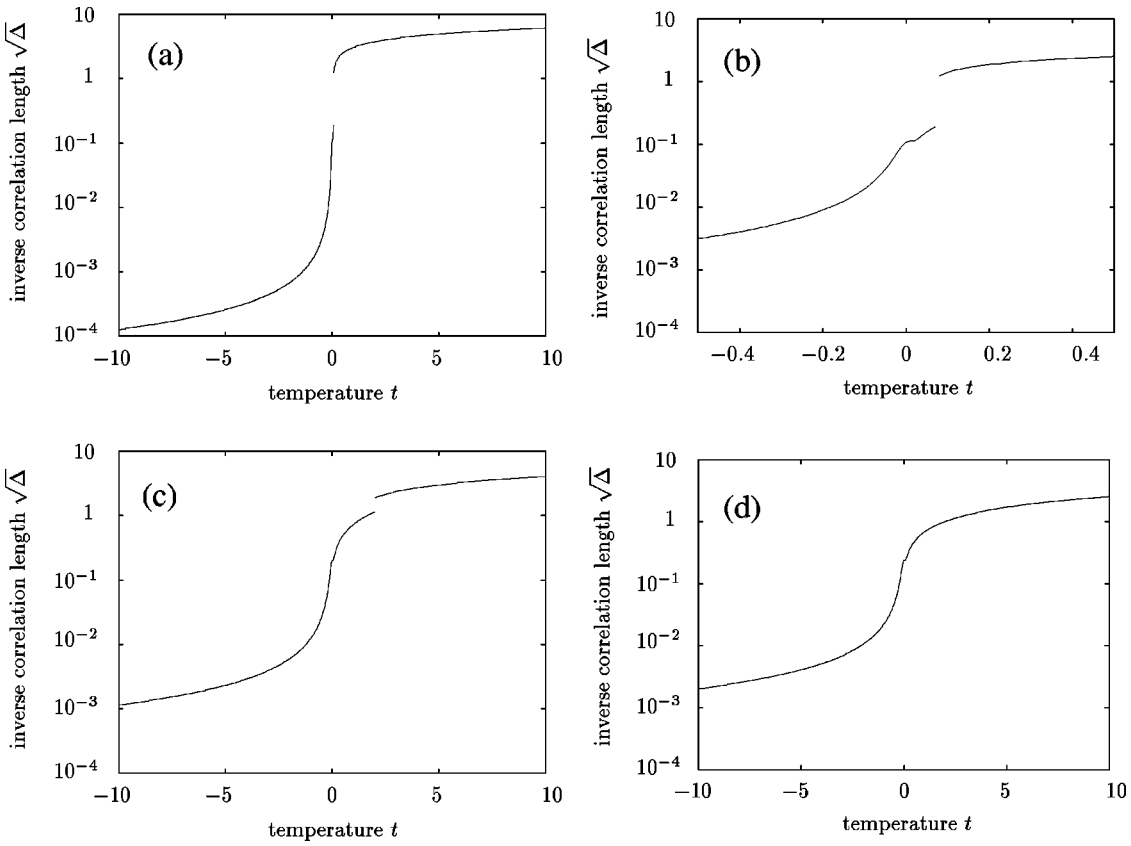

FIG. 11. Inverse correlation length $\sqrt{\Delta}$ vs temperature t for different q_0. (a) $q_0=0.2$. (b) A close-up of (a) reveals a clear jump of the inverse correlation length at $t\approx 0.1$, indicating a first-order phase transition. (c) $q_0=0.6$. The jump has decreased compared to $q_0=0.2$. (d) $q_0=0.8$. The function is now continuous.

VIII. DISCUSSION

We have shown that the cumulant expansion is an appropriate method to treat order parameter fluctuations in chiral-nematic liquid crystals. The Brazovskiĭ theory used before in similar systems [15] cannot be applied to blue phases. Within a first-order expansion, it has been proven that the cubic O^5 structure is only present for very small values of the clearing-point temperature T_c corresponding to the parameter $\alpha \lesssim 0.075$.

For high chiralities BP II vanishes, in agreement with the experiment. This is already the case for mean-field calculations at $\kappa \approx 12$. The role of fluctuations is to shift the point where O^2 disappears to lower chiralities.

We have presented various phase diagrams of the blue phases under the presence of fluctuations. The phase diagram which agrees best with the experiment has been obtained for $\alpha=0.2$ [Figs. 6(a) and 7]. The correlation length or, respectively, susceptibility of the alignment tensor field shows a smooth transition between two isotropic phases, a highly correlated metastable one, which we interpret as BP III, and a weakly correlated stable one which is the ''true'' isotropic phase.

In a simplified model we have investigated isostructural transitions within the isotropic phase using a chiral ϕ^4 theory and a third-order cumulant expansion. We could prove the existence of a first-order phase transition between two isotropic phases which ends at a critical point when the chirality is increased. The appropriate physical quantity to be used as an order parameter is the susceptibility of the alignment tensor field. It leads to the unique situation that the fluctuations of the order parameters of the ordered system act as order parameter of the disordered system. Fluctuations of the new order parameter at the critical point have to be described by methods similar to these as given in Ref. [18].

One serious limitation is the use of a Gaussian trial Hamiltonian, since all odd order correlation functions vanish *a priori*. It cannot be estimated how strongly it influences the results. On the other hand, there is no method known to date, which can handle such expressions correctly, apart from Monte Carlo path integrations.

Another limitation is the neglection of modes $m\neq 2$. We are sure, however, that the results are not seriously touched,

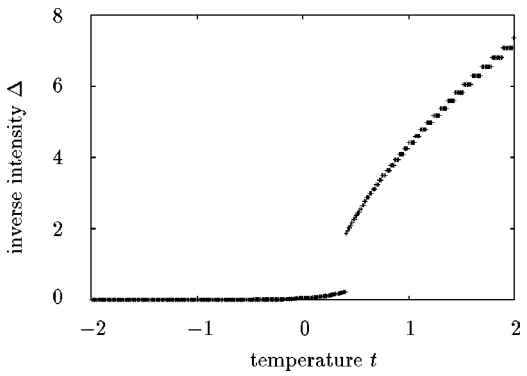

FIG. 12. Inverse intensity Δ (on a linear scale) vs temperature t for $q_0=0.4$. This allows for direct comparison with the experimental light scattering data at the isotropic–BP III transition [6].

because we have shown the dominance of the $m=2$ modes in the mean field. The strongest fluctuating modes should also be the $m=2$ modes since they can be treated as perturbations of the equilibrium modes. For the behavior of the isotropic phase nothing new has to be expected when extending the first-order theory to other modes.

For increasing chirality the order of appearance of the cubic phases is still first O^2, then O^8, in disagreement with experiment. It may be resolved by use of higher-order approximations which possibly enhance the fluctuations at small chiralities.

ACKNOWLEDGMENTS

This project was supported by the Deutsche Forschungsgemeinschaft under Grant No. Tr 154/15-1. We thank A. Rüdinger for useful discussions.

[1] V. A. Belyakov and V. E. Dmitrienko, Usp. Fiz. Nauk **146**, 369 (1985) [Sov. Phys. Usp. **28**, 535 (1985)]; H. Stegemeyer, Th. Blümel, K. Hiltrop, H. Onusseit, and F. Porsch, Liq. Cryst. **1**, 3 (1986); D. C. Wright and N. D. Mermin, Rev. Mod. Phys. **61**, 385 (1989); P. P. Crooker, Liq. Cryst. **5**, 751 (1989); T. Seideman, Rep. Prog. Phys. **53**, 659 (1990).

[2] R. Barbet-Massin and P. Pieranski, J. Phys. Colloq. **C3**, C3-61 (1985).

[3] S. R. Renn and T. C. Lubensky, Phys. Rev. A **41**, 4392 (1988); J. W. Goodby, M. A. Waugh, S. M. Stein, E. Chin, R. Pindak, and J. S. Patel, Nature (London) **337**, 449 (1989).

[4] B. Pansu, M. H. Li, and H. T. Nguyen, J. Phys. II **7**, 751 (1997).

[5] J. B. Becker and P. J. Collings, Mol. Cryst. Liq. Cryst. **265**, 163 (1995).

[6] E. P. Koistinen and P. H. Keyes, Phys. Rev. Lett. **74**, 4460 (1995).

[7] Z. Kutnjak, C. W. Garland, J. L. Passmore, and P. J. Collings, Phys. Rev. Lett. **74**, 4859 (1995).

[8] N. A. Clark, S. T. Vohra, and M. A. Handschy, Phys. Rev. Lett. **52**, 57 (1984); P. E. Cladis, P. Pieranski, and M. Joanicot, *ibid.* **52**, 542 (1984); R. N. Kleiman, D. J. Bishop, R. Pindak, and P. Taborek, *ibid.* **53**, 2137 (1984).

[9] H. Stark and H.-R. Trebin, Phys. Rev. E **51**, 2316 (1995).

[10] H. Stark and H.-R. Trebin, Phys. Rev. E **51**, 2326 (1995).

[11] H. Grebel, R. M. Hornreich, and S. Shtrikman, Phys. Rev. A **28**, 1114 (1983); **30**, 3264 (1984).

[12] L. Longa, W. Fink, and H.-R. Trebin, Phys. Rev. E **50**, 3841 (1994).

[13] L. Longa and H.-R. Trebin, Phys. Rev. Lett. **71**, 2757 (1993); J. Englert, L. Longa, and H.-R. Trebin, Liq. Cryst. **21**, 243 (1996).

[14] D. Bensimon, E. Domany, and S. Shtrikman, Phys. Rev. A **28**, 427 (1983).

[15] E. I. Kats, V. V. Lebedev, and A. R. Muratov, Phys. Rep. **228**, 1 (1993).

[16] D. K. Yang and P. P. Crooker, Phys. Rev. A **35**, 4419 (1987).

[17] A. Hauser, M. Thieme, A. Saupe, D. Krüerke, and G. Heppke, J. Mater. Chem. **7**, 2223 (1997).

[18] T. C. Lubensky and H. Stark, Phys. Rev. E **53**, 714 (1996).

[19] M. A. Anisimov, V. A. Agayan, and P. J. Collings, Phys. Rev. E **57**, 582 (1998).

[20] L. Longa, J. Englert, and H.-R. Trebin, in *Proceedings of the LMS Symposium on Mathematical Models of Liquid Crystals and Related Polymeric Systems* (Cambridge University Press, Cambridge, England, 1995).

[21] S. A. Brazovskĭ, Zh. Éksp. Teor. Fiz. **68**, 175 (1975) [Sov. Phys. JETP **41**, 85 (1975)]; S. A. Brazovskĭ and S. G. Dmitriev, *ibid.* **69**, 979 (1975) [**42**, 497 (1975)].

[22] J. Englert, *Über den Einfluß von Fluktuationen auf die Chiral-Nematischen Blauen Phasen* (Shaker Verlag, Aachen, 1998).

[23] P. G. de Gennes and J. Prost, *The Physics of Liquid Crystals*, 2nd ed. (Clarendon Press, Oxford, 1993).

[24] N. Goldenfeld, *Lectures on Phase Transitions and the Renormalization Group*, Frontiers in Physics Vol. 85 (Addison-Wesley, Reading, MA, 1992).

[25] A. V. Dobrynin, J. Phys. I **5**, 1241 (1995).